**International Journal of Pharmacy and Pharmaceutical Research (IJPPR)**
Volume 31, Issue 12, December 2025 **ijppr.humanjournals.com** ISSN: 2349-7203

# The Corrosion Resistance of Semi-Solid Welded Al-Mg-Si Alloy

**A.Geetha[a], C.Jeevarathinam[b], M.Chithralekha[c], G.V.Pandian[d]**

[a]Department of Chemistry, Tagore Institute of Engineering and Technology, Salem, Tamilnadu, INDIA.
bDepartment of Chemistry, Raak Arts and Science College, Perambai, Pondicherry, INDIA.
[c]Department of Chemistry, D.G. Government Arts College for Women, Mayiladuthurai, Tamilnadu, INDIA.
[d]Department of Chemistry, TBML College, Porayar, Tamilnadu, INDIA.

Received: 09 November 2025 Revised: 25 November 2025 Accepted: 10 December 2025

**ABSTRACT**

The Al-Mg-Si alloy is widely recognized as a valuable engineering material, particularly in the aerospace sector, due to its excellent strength-to-weight ratio. Recent advancements have enhanced the welding of these alloys through a process known as Thixo-Joining or semi-solid welding. This study investigates the corrosion resistance of Al-Mg-Si welds under both acidic and marine conditions. Welds were produced at various temperatures ($34^0$C), $100^0$C, $200^0$C and $300^0$C prior to environmental exposure. Standardized test coupons were subjected to weight loss measurements using the gravimetric method and electrochemical testing via linear polarization to evaluate corrosion behavior. Results showed that corrosion resistance improved with the welded samples compared to the parent material (PM), particularly when analyzed using the gravimetric method. Additionally, the formation of globules at the weld sites acted as crack arresters, enhancing resistance to degradation. These findings suggest that Thixo-Joining contributes to superior performance in harsh environmental conditions.

**Keyboards:** Corrosion resistance, Thixo-Joining, Exfoliation, welding performance

## INTRODUCTION

Fusion welding, a widely used conventional joining technique, is often accompanied by high temperature gradients, leading to rapid solidification and thermal stress. This can result in segregation phenomenon (Kou, 2003). The welded interface typically has a dendritic morphology, and the natural course of solidification often introduces structural defects such as shrinkage, porosities, and alloying element loss, ultimately producing a non- uniform micro structure (Callister and Rethwisch, 2011). To overcome these drawbacks, advanced techniques have been developed. One such promising method is the Semi-Solid Process (SSP), also known as thixo-joining. This process occurs in a semi-solid state, where the mechanisms of solidification and heat transfer are distinctly different from those in conventional welding (Mohammed ***et al.,*** 2017). The semi-solid joining technique, often referred to as thixo-joinig or thixo-forming, is grounded in the principles of Semi-Solid Metal processing (SSP) (Kirkwood, 1994). It enables the joining of metals when they are partially solid and partially liquid (Seo, and Kang, 2001). The unique rheological behavior of materials in this state makes it possible to achieve reliable joints. A key goal in SSP is to produce a globular rather than a dendritic solid structure within the liquid matrix (Mian 2016). Another strategy for obtaining a globular microstructure is semi-solid thermal transformation, which involves heating the material and holding it within the semi-solid temperature range for a specific duration, thereby promoting a more uniform structure (Wang ***et al.,*** 2004). In recent years, there has been a growing demand for lightweight and high-strength sheet metals, particularly aluminium alloys, across sectors such as aerospace, automotive and aircraft manufacturing. This increasing preference is largely due to their favorable strength-to-weight ratio, excellent ductility, and superior resistance to corrosion and cracking, especially in harsh environmental conditions (Polmear, 1995).

The rigid joining of materials is a fundamental process in both manufacturing and assembly. Aluminum alloys are often joined using conventional fusion welding techniques. These include tungsten inert gas (TIG) welding, gas metal arc welding (GMAW or MIG) and friction stir welding - all of which are commonly employed for aluminium due to their effectiveness (Kou, 2003). Aluminium and its alloys are especially well -suited for fusion welding and are extensively used in serial production. Continuous advancements in welding equipment, tools and materials have facilitated the broader adoption of specialized fusion welding methods tailored for aluminium joining (Callister and Rethwisch, 2011). Achieving high-strength welds in aluminium alloys largely depends on the metallurgical transformations occurring in the weld zone. These processes involve the fusion of the base metal and the solidification of the molten weld pool. The solidification behavior significantly influences weld quality. Typically, the solidification structure in aluminium welds tends to be dendritic. This, along with the progression of solidification fronts, can lead to defects, such as shrinkage porosity. Such micro structural imperfections often result in welds with mechanical properties that are inferior to those of the original cast or base metal (Gene Mathers, 2002). The Semi-Solid Processing (SSP) technique is emerging as a

promising approach for developing lightweight, high-strength components for engineering applications. This method requires specific material properties to achieve optimal results (Adebayo A.V, 2000). Although numerous studies have highlighted the benefits of SSP in enhancing mechanical characteristics, less attention has been paid to its behaviour in corrosive environments. Therefore, the present study focuses on evaluating the corrosion susceptibility of Al-Mg-Si alloy under both acidic and marine conditions.

## METHODOLOGY

The materials used for this study included aluminium alloy 6063 (Al-Mg-Si system). A steel plate served as a metallic mould to hold the Al-Mg-Si alloy work piece during casting. The chemical composition of the alloy is presented in Table 1. The as-cast alloy samples, with dimensions 45mm x 20mm x 15mm, were machined into a single V-edge joint configuration (Figure 1). An induction heating coil was employed to heat the joint area to various target temperatures - ambient ($34^0$C), $100^0$C, $200^0$C and $300^0$C. During heating, the semi-solid slurry was mechanically agitated to maintain uniform temperature and achieve the desired semi-solid state for the welding process.

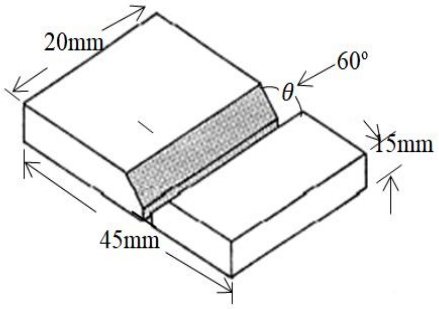


**Figure 1: Schematic representation of the V-Joint configuration used for sample preparation.**

**Table 1: Elemental analysis of the Aluminium Alloy expressed in weight percent (wt %)**

| S.NO | ELEMENTS | WEIGHT % |
|---|---|---|
| 1 | Si | 0.509 |
| 2 | Fe | 0.829 |
| 3 | Cu | 0.0548 |
| 4 | Mn | 0.0412 |
| 5 | Mg | 0.242 |
| 6 | Cr | 0.0164 |
| 7 | Ti | 0.0137 |
| 8 | Ca | 0.0019 |
| 9 | Ni | 0.0065 |
| 10 | Al | 98.2 |
| 11 | Zn | 0.0757 |
| 12 | Zr | 0.00080 |
| 13 | Pb | 0.0030 |

## CASTING PROCEDURE

The semi-solid slurry was poured continuously into the preheated as-cast aluminium alloy samples held at varying temperatures: $34^0$C (room temperature), $100^0$C, $200^0$C and $300^0$C. The samples were positioned in a specially designed metallic mould to ensure consistent flow and solidification. The casting was performed under optimized parameters, including a pouring temperature of $580^0$C, a mould slope length of 400 mm, and an inclination angle of 600 as shown in Figure 2. (Mohammed, ***et al.,*** 2017)

International Journal of Pharmacy and Pharmaceutical Research (IJPPR)
Volume 31, Issue 12, December 2025 ijppr.humanjournals.com ISSN: 2349-7203

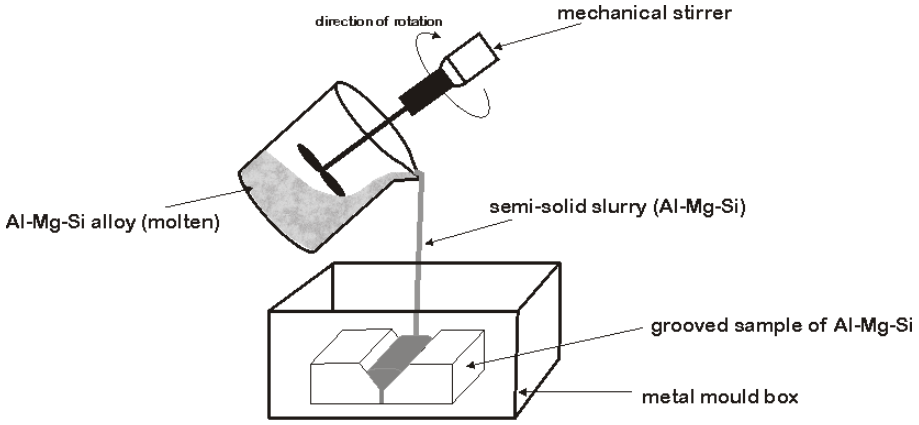


**Figure 2: Schematic Diagram Showing the Principle of Semi-Solid Welding of Al-Mg-Si Alloy**

## CORROSION TEST

Marine environments pose significant challenges to materials due to their aggressive corrosive nature. As such, evaluating the corrosion resistance of materials used in these conditions is critical to ensuring structural integrity and service life Adeosun ***et al.,*** (2012). In this study, the corrosion susceptibility of welded aluminium alloy specimens was assessed, with particular focus on the as-cast and retrogression zones. The evaluation was conducted using the exfoliation corrosion (EXCO) test and potentio dynamic electrochemical analysis, following the ASTM G34 standard methodology.

## EXFOLIATION CORROSION TESTING

The exfoliation corrosion (EXCO) test was employed to examine the surface degradation characteristics of Al–Mg–Si alloys under simulated industrial and marine conditions. This method evaluates the susceptibility of the material to surface layer detachment (exfoliation) due to aggressive environmental exposure. The test solution was prepared by dissolving 5 g of $KNO_3$ and 9 ml of $HNO_3$ in 300 ml of distilled water, creating a corrosive medium that replicates harsh service environments. Corrosion progression was quantified using gravimetric analysis. In this approach, the weight loss of the test specimens was measured before and after exposure. After each exposure phase, specimens were cleaned with distilled water, air-dried, and reweighed to determine the extent of material loss. The corrosion rate was then calculated using the following equation:

$$\text{Corrosion Rate} = \frac{\text{(Weight Loss (mg) x K)}}{\text{Density of Test Specimen x Area of Test Specimen (cm}^2\text{) x Exposure Time (hr)}}$$

$$\text{Corrosion Rate} = \frac{W \times K}{A \times \rho \times T} \quad \text{(ASTM } G_1/4\text{)} \qquad \text{---(1)}$$

Where,

W: is Weight Loss is the difference in weight of the specimen before and after the monitoring phase,expressed in milligrams (mg).

K: is a constant for converting the units ($3.5x10^4$x $Dg/m^2h$)

ρ: Density of Test Specimen is the density of the material being tested.

A: Area of Test specimen is the surface area of the specimen exposed to the corrosive environment, expressed in square centimeter ($cm^2$).

T: Exposure Time is the duration of the monitoring phase, expressed in hours (hr).

The gravimetric method is a widely accepted technique for evaluating the corrosion behaviour of aluminium alloys under various environmental conditions. In this study, the exfoliation corrosion (EXCO) test was performed in accordance with ASTM G34 standards, which are typically applied to aluminium alloys in the 6XXX and 7XXX series. The test simulates aggressive corrosive environments such as marine or industrial settings by immersing specimens in a chemically prepared solution for 72 hours. To

replicate harsh exposure conditions, the test solution was formulated using highly corrosive agents diluted with deionised water. The specimens, sized 43 × 20 × 15 mm, were placed in non-reactive plastic containers. Prior to testing, the surfaces were decreased with lamp oil, rinsed, and their initial weights recorded. A solution containing potassium nitrate and nitric acid was prepared, maintaining a volume-to-metal surface area ratio of approximately 320 ml per specimen. The immersion was conducted at 32 °C with a solution pH of 6.4 for a total duration of 72 hours. At regular intervals, the specimens were visually inspected for signs of exfoliation. Corrosion severity was assessed using a standardized rating system by comparing the exposed samples with reference photographs. Photographic documentation was performed using a metallurgical microscope.

Upon completion of the test period, the specimens were gently rinsed with warm water, dried, and weighed again. The corrosion rate was calculated using the weight loss data before and after exposure, based on the standard corrosion rate formula (Equation 1).

**POTENTIODYNAMIC ELECTROCHEMICAL MEASUREMENT TECHNIQUE:**

The electrochemical corrosion behaviour of the samples was investigated in a simulated marine environment using a 3.5 wt.% sodium chloride (NaCl) solution. Potentiodynamic polarization tests were conducted to assess the corrosion resistance, and the results were compared with those obtained from the exfoliation corrosion tests (Lian ***et al.,*** 2019; Zhao ***et al.,*** 2021). All electrochemical measurements were carried out at room temperature (approximately 34 °C) using an Auto Lab potentio stat system (Khadom ***et al.,*** 2020; Umoren ***et al.,*** 2021). Prior to polarization, the specimens were immersed in the electrolyte solution for a sufficient duration to stabilize at the open circuit potential (OCP). The potentiodynamic scans were then conducted at a rate of 1 mV/s, starting from −250 mV below the OCP and progressing to +250 mV above it. Following each scan, the electrolyte solution was replaced with a fresh one. The tested specimens were mechanically polished, rinsed with distilled water, and cleaned with acetone to remove any surface residues that might interfere with subsequent measurements.

**RESULTS AND DISCUSSION**

**Exfoliation Corrosion Test**

After exposure to the corrosive environment, the specimens were visually examined to assess the extent of surface degradation. The visual inspection did not indicate significant corrosion at the fusion zones. The classification and severity of exfoliation were determined using the standard visual rating guide, as outlined in Table 2, in accordance with ASTM G34 procedures.

**Table 2: Visual Rating Guide for the Samples**

| Classifications | Code |
|---|---|
| No appreciable attack | N |
| Pitting | P |
| Exfoliation | EA,EB,EC,ED |

N- No appreciable attack

P- Give the appearance of incipient exfoliation.

EA- (superficial): Tiny Blisters, Thin Silvers, Flakes or Powder, with only slight Separation of Metal

EB- (Moderate): Notable Layering and Penetration into the Metal.

EC- Penetration to a Considerable Depth into the Metal.

ED- (very severe): Similar to EC Except for Much Greater penetration and loss of metal.

Micrographs of the Exfoliation Corrosion Test

Figure: 3 presents the micro structural features of the as-cast Al–Mg–Si alloy following exposure to a corrosive environment. The micrographs reveal a coarse and non-uniform grain structure, along with visible casting defects such as blowholes, which likely facilitated the penetration of corrosive agents. These effects became more severe after 72 hrs of exposure, where deeper and more widespread cavities were observed in Figure 4. Post-welding micro structural analysis showed significant improvements. The weld zone exhibited a finer and more uniform grain structure, with fewer casting-related defects compared to the untreated sample. This refinement was especially evident in the samples welded at elevated temperatures, as shown in Figures 5 and 6. At 200 °C (T2) and 300 °C (T3), the micro structures demonstrated reduced porosity and enhanced grain refinement, suggesting that increased welding temperatures contribute to improved structural integrity and resistance to corrosion-induced damage.

International Journal of Pharmacy and Pharmaceutical Research (IJPPR)
Volume 31, Issue 12, December 2025 ijppr.humanjournals.com ISSN: 2349-7203

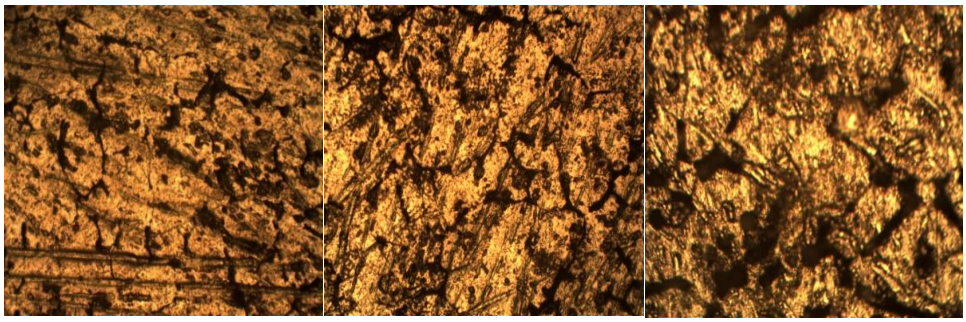

**Figure 3: As-cast Micrographs of Exco Test after (a) 24 hours (b) 48 hours and (c) 72 hours showing the Prevalence of Increasing Depth Pits on the Specimen's Mag:x200**

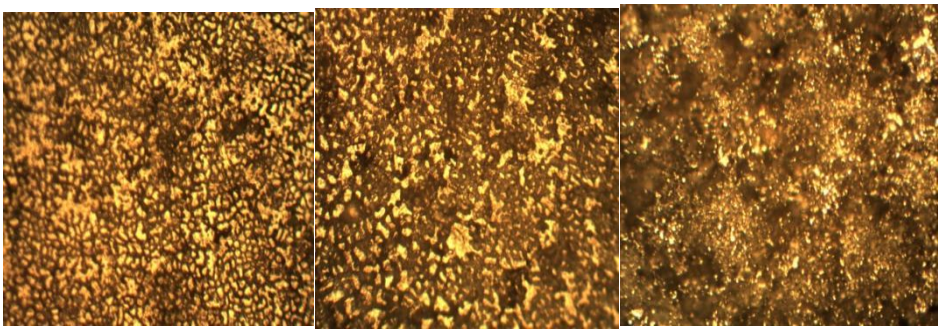

**Figure 4: Micrographs of weld zones of Exco test at 100◦C after (a) 24 hours (b) 48 hours and (c) 72 hours showing a trace of crevice corrosion at the grain boundaries. Magx200**

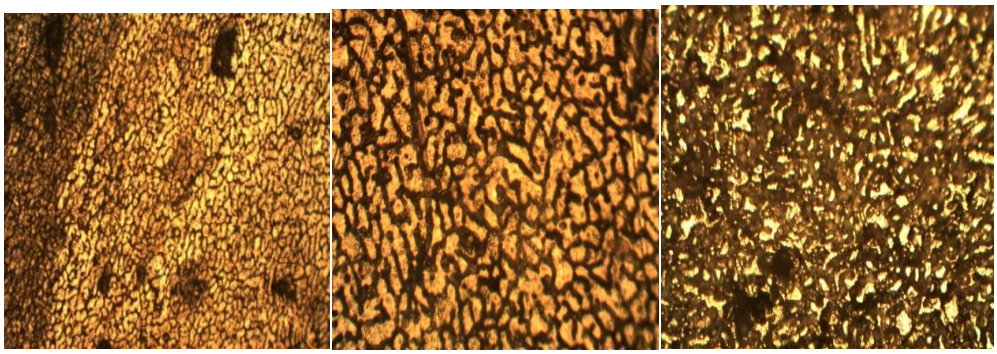

**Figure 5: Micrographs of weld zones of Exco test at 200◦C after (a) 24 hours (b) 48 hours and (c) 72 hours showing a Pit corrosion. x200**

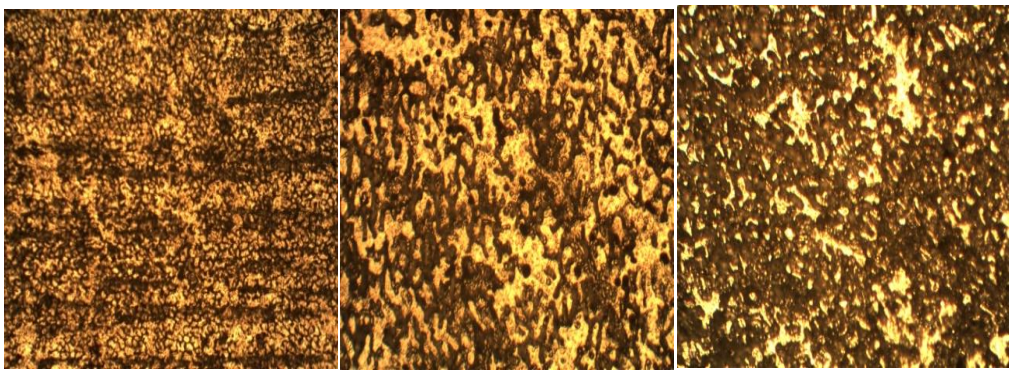

**Figure 6: Micrographs of weld zones of Exco test at 300◦C after (a) 24 hours (b) 48 hours and (c) 72 hours showing a trace crevice corrosion attack. x200**

The corrosion micrograph of $T_2$, presented in Figure 5, reveals a coarse microstructure in the weld zone, which increases its vulnerability to corrosion. This observation aligns with the findings of Yu ***et al.,*** (2002), who reported that semi-solid microstructures exhibit greater resistance to both general corrosion and stress corrosion cracking. When comparing semi-solid and low-pressure die-cast components, they also noted a higher degree of pitting and overall corrosion in conventionally cast products compared to cast counterparts.

**CORROSION RATE: GRAVIMETRIC ANALYSIS**

The corrosion rate of each sample was determined to evaluate the extent of material degradation. This was based on the total surface area and the mass loss after exposure to corrosive conditions. The procedure followed ASTM G1 standards. Figure 7 illustrates the variation in corrosion rate corresponding to different treatment durations (24 hrs, 48 hrs, and 72 hrs). It was observed that all samples displayed a clear sinusoidal pattern in corrosion behavior, irrespective of the temperature conditions applied during testing. The control sample maintained a consistently low corrosion rate, suggesting good resistance to corrosion over time. At ambient temperature ($T_a$), the corrosion rate initially rose sharply, peaking near 2°C, before declining rapidly. This indicates that corrosion is highly sensitive to changes in temperature. The $T_1$ sample followed a trend similar to $T_a$, with a notable peak around 2°C. However, the overall corrosion rate for $T_1$ was higher than that of the control sample. The $T_2$ sample exhibited a bimodal distribution, with significant peaks around 2°C and 4°C, implying that factors beyond temperature alone influence the corrosion process. On the other hand, the $T_3$ sample displayed a low and stable corrosion rate, comparable to the control, indicating that the temperature fluctuations in this range had minimal effect on corrosion behavior. Overall, the graph highlights the significant influence of temperature variations on the corrosion rate of the samples, with the most notable changes observed around 2 °C and 4 °C. These findings offer valuable insights into corrosion behavior under varying temperature conditions, which are essential for developing effective strategies to manage corrosion across different applications. The results from the corrosion rate analysis align well with existing literature regarding the impact of temperature on material corrosion. A study by Loto ***et al.,***(2017) demonstrated that corrosion rates increased markedly with temperature, showing a peak around 30 °C. This observation is consistent with the present study, where significant changes were recorded near 2 °C and 4 °C. The authors attributed this trend to enhanced electro chemical reactions and the formation of corrosion products at elevated temperatures. Similarly, research by Kemani and Morshed (2003) examined the influence of temperature on steel corrosion in oil and gas production environments. They reported that corrosion rates typically rise exponentially with increasing temperature due to accelerated cathodic and anodic reactions, as well as increased solubility of corrosion products. Furthermore, Oguzie, ***et al.,*** (2019) investigated the corrosion behavior of aluminum alloys in acidic media and reported a bimodal distribution of corrosion rates across varying temperatures. The authors attributed this phenomenon to the complex interaction of factors such as the dissolution of protective oxide layers and the formation of new corrosion products over different temperature ranges.

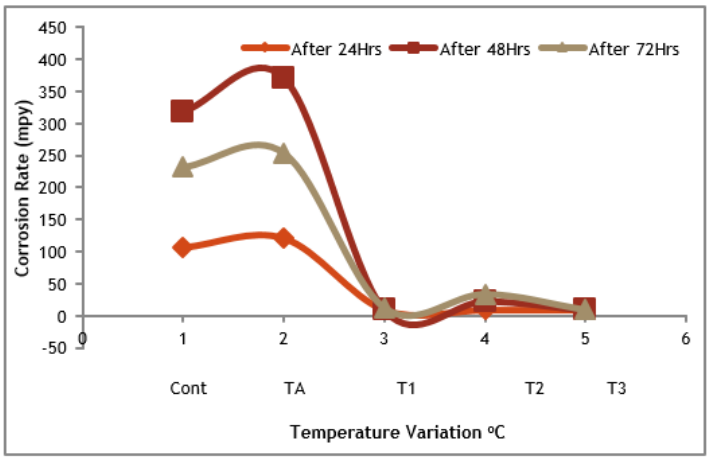


**Figure 7: Gravimetric Trend for the Corrosion of Al-Mg-Si Alloy Using Exfoliation Corrosion Technique**

**Linear Polarization Test**

The graphs presented in Figures 8(a) and 8(b) illustrate the Tafel polarization curves for a control sample and three different treated samples (T1: NaCl, T2: NaCl + acid, and T3: NaCl + acid + elevated temperature). These samples were exposed to a 3.5% NaCl solution and acidic environments under varying conditions. The polarization curves for the Al-Mg-Si alloys reveal a strong correlation between increased corrosion activity and exposure to acidic and marine environments. The results indicate that as the treatment temperature increases, the corrosion resistance of the alloy decreases accordingly. This observation is consistent with the

gravimetric analysis presented in Figure 7, which also shows increased mass loss under harsher conditions, thereby confirming the trend in corrosion behavior across different treatment environments.

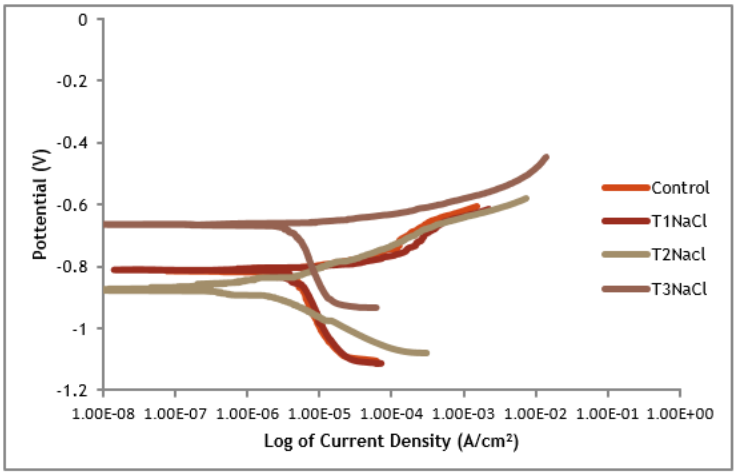


**Figure 8 (a): Polarization curves of Al-Mg-Si alloy Exposed to a 3.5%NaCl Solution**

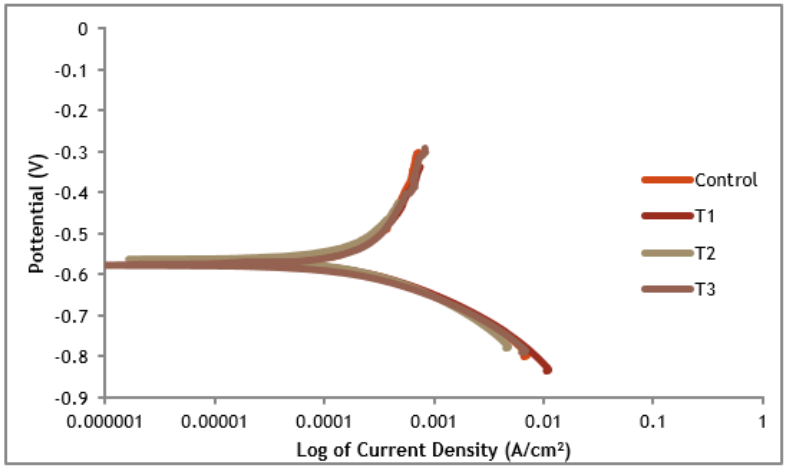


**Figure 8(b): Tafel Polarization curves of Al-Mg-Si alloy Exposed to Acidic Environment**

The control sample demonstrated the most noble corrosion potential, indicating superior corrosion resistance compared to the treated samples. Correspondingly, its corrosion current density was relatively low, suggesting a reduced rate of corrosion. In contrast, the T1 sample exhibited the most cathodic (negative) corrosion potential, signifying a higher susceptibility to corrosion. This sample also recorded the highest corrosion current density, indicating a significantly elevated corrosion rate relative to the control. Sample T2 (NaCl) displayed a more negative corrosion potential than the control, though less negative than T1(NaCl). Its corrosion current density was also lower than that of T1 but remained higher than the control sample, suggesting a moderate corrosion rate. For sample T3 (NaCl), the corrosion potential was more positive than both T1 (NaCl) and T2 (NaCl), indicating improved corrosion resistance. The current density recorded for T3 was lower than both T1 and T2 samples but still exceeded the value for the control sample, indicating an intermediate level of corrosion resistance. The Tafel polarization curves clearly demonstrate the impact of different treatment conditions (T1, T2, and T3) on the corrosion behavior of Al-Mg-Si alloys. The control sample exhibited the best corrosion resistance, while the T1 treatment condition resulted in the poorest resistance. Samples T2 and T3 showed moderate corrosion behavior, lying between the extremes of the control and T1. These findings align with existing literature on the effects of temperature and chemical exposure on the corrosion performance of aluminum alloys. For example, Xiao ***et al.,***(2020) reported that increased exposure to elevated temperatures in saline environments led to a shift in corrosion potential toward more noble values and a reduction in corrosion current density, indicative of improved resistance. This trend corresponds well with the performance of the control and T2 samples in the current study.

Several studies have investigated the influence of sodium chloride (NaCl) concentration on the corrosion behavior of aluminum-magnesium-silicon (Al-Mg-Si) alloys. Abdallah ***et al.,*** (2019) reported that increasing NaCl concentration results in a more negative

corrosion potential and elevated corrosion current density, indicating higher susceptibility to corrosion. This trend was particularly evident in the T1(NaCl) and T2(NaCl) sample groups. In addition, Zheludkevich ***et al.,*** (2005) emphasized the significance of understanding how temperature, chemical composition, and surface modifications interact to affect the corrosion resistance of aluminum alloys. Their review highlighted the importance of using advanced characterization techniques, such as Tafel polarization, to guide alloy design and surface treatment strategies aimed at enhancing corrosion resistance. Understanding these factors is essential for predicting and improving the corrosion performance of aluminum alloys under varying environmental conditions. Such insights enable the development of optimized materials and processing techniques to enhance corrosion resistance.

**CONCLUSION**

This study evaluated the impact of the semi-solid welding technique on the corrosion resistance of Al-Mg-Si alloy in both acidic and marine environments. The alloy was welded under semi-solid conditions at various temperatures (34°C, 100°C, 200°C, and 300°C). Standardized methods were employed to prepare the test samples, which were then analyzed using weight loss (gravimetric) and linear polarization techniques. The main findings are summarized as follows: Semi-solid welding presents a promising alternative to conventional fusion welding for Al-Mg-Si alloys. It has the potential to minimize casting-related defects typically encountered in fusion welding processes. The exfoliation corrosion analysis (based on weight loss measurements) indicated that the globular micro structure produced during semi-solid welding acts as an effective barrier against crack propagation, thereby reducing corrosion vulnerability in both marine and industrial environments. In comparison, the base metal and joints fabricated at room temperature exhibited higher susceptibility to corrosion. These results were further corroborated by Tafel polarization data. Overall, the semi-solid welding method significantly enhances the corrosion resistance of Al-Mg-Si alloys. The development of a refined globular micro structure during welding is a key factor in improving performance under aggressive environmental conditions.

**REFERENCES:**

1. Abdallah, M., Zaafarany, I., Fawzy, A., Fouda, A.S.., & Asghar, B.H. (2009). Corrosion inhibition of aluminium in hydrochloric acid solution using some organic compounds. International Journal of Electro chemical Science, 14, 1507-1525.
2. Adebayo A.V (2000): Basic and Benefits os Semi-Solid Metallurgy. Journal of Research in Technology and Engineering Management, Vol.2, No.1, Pp25-29.
3. Adeosun, S.O., Sekunowo, O.I., Balogun, S.A. and Obiekaa, V.D. (2012): Corrosion Behaviour of Heat-Treated Aluminium-Magnesium Alloy in Chloride and EXCO Environments: International Journal of Corrosion Volume 2, Article id 927380, P1-9.
4. ASTM G34-01 (2013) Standard Test Method for Exfoliation Corrosion Susceptibility in 2XXX and 7XXX Series Aluminium Alloys (EXCO Test) (West Conshohocken, PA.
5. AST, G5. (2014) Standard reference test method for making potentiostatic and potentiodynamic anodic polarization measurements, (EXCO Test) (West Conshohocken, PA.
6. Ankur Choudhury, Abjhimanuy Gopakumar, Athul KP, DR Adinath and Mrudula Prashanth (2017). Experimental analysis of Exfoliation rate on Aluminium alloy Al7010. IOP Conference Series: Materials Science and Engineering; 225 (2017)012037
7. Baur J. (1998): Thixo-forging of Cu-Zn Alloy, proceeding 5th International Conference on Semi-Solid processing of Alloys and Composities, pp 299-306, Golden, colo, USA.
8. Callister, W. D., and Rethwisch, D. G. (2011). Materials Science and Engineering: An Introduction (9th ed.). John Wiley & Sons.
9. Davis, J.R. (2000). Corrosion of aluminum and aluminum alloys. ASM International.
10. Gene Mathers (2002): The Welding of aluminium and its alloys, woodhead Publishing Limited, Abington hall, Abington Cambridge, England.
11. Kermani, M. B., and Morshed, A. (2003).Carbon dioxide corrosion in oil and gas production: a compendium. Corrosion, 59(8), 659-683.
12. Khadom, A. A., Yaro, A. S., AlTaie, A. S., and Deyab, M. A. (2020). Corrosion inhibition of aluminium Metal (AA2024) in hydrochloric acid by the ionic liquid 1-ethyl-3-methylimidazolium ethyl sulphate. Journal of Materials Research and Technology, 9(2), 1931-1943.
13. Kirkwood, D. H. (1994). Semisolid metal processing. *International Materials Reviews,* 39(5), 173-189.
14. Kou, S. (2003). Welding Metallurgy (2nd ed.). John Wiley & Sons.
15. Lian, J. S., Rao, G. A., Ouyang, W. H., and Blandin, W. J. (2019). Exfoliation corrosion testing of 7075 .
16. Loto, C. A. (2017). The effect of temperature on the corrosion inhibition of mild steel in seawater. Journal of Materials and Environmental Science, 8(4), 1475-1487.
17. Mian, W. S. (2016): Investigation of semi-solid metal processing route; Thesis submit Master of Engineering School of Mechanical & Manufacturing Engineering Dublin University.
18. Mohammed, M.N., Omar, M. Z., Salleh, M. S., Alhawari, K. S., Kapranos, P. (2017):Effect of Welding Parameters on Microstructure Properties of Semi-Solid Welded D2 Cold-Work Tool Steel Joints, *Journal of Management and Science University* –Vol. 14, No 2.
19. Oguzie, E. E., Onuoha, G. N., Onuchukwu, A. I., & Daya, V. E. (2019). Temperature effect on the corrosion inhibition of aluminum in acidic media. Materials Chemistry and Physics, 120(3), 571-575.

20. Polmear, A. J. (1995). Light alloys: Metallurgy of the light metals (3rd ed.). Arnold.
21. Seo, P. K., and Kang, C. G. (2001). Prediction of material behaviour in semi-solid die casting process using a viscoplastic constitutive equation. *Journal of Materials Processing Technology*, 111(1-3), 44-54.
22. Umoren, S. A., Obot, I. B., Madhankumar, A., and Gasem, Z. M. (2021). Performance evaluation of Aluminium alloy AA8011 in chloride and sulphate media: Influence of thio-semi-carbazone derivatives. Journal of Adhesion Science and Technology, 35(9), 998-1020.
23. Wang, H., Davidson, C. J. and St. John, D. H. (2004): Semisolid Microstructural Evolution of Al-Si-Mg using partial Re-melting, Mater. Sci. Vol. 368, Issues 1-2, pp.159-167.
24. Xiao, K., Dong, C., Dong, L., Kong, D., Li, X., & Wang, L. (2020). Effect of temperature on the corrosion behavior of Al-Mg-Si alloy in 3.5% NaCl solution. Journal of Materials Engineering and Performance, 29(5), 3105-3115.
25. Yu Y., Kim S., Lee Y. and Lee J. (2002): Phenomenological Observations on Mechanical and Corrosion Properties of Thixo-formed Alloys: A comparison with Permanent Mold Cast 357 Alloys. Metall. Trans, 33,Pp 1339 – 1412.
26. Zhao, H., Wang, X., Zhang, Q., and Jiang, X. (2021). Exfoliation corrosion behaviour of 2024 aluminium alloy in seawater with different sodium chloride concentrations. Materials Today: Proceedings, 40, 356-361.
27. Zheludkevich, M. L., Salvado, I. M. and Ferreira, M. G. (2005). Sol-gel coatings for corrosion protection of metals. Journal of Materials Chemistry, 15(48), 5099-5111.

How to cite this article:
A.Geetha et al. Ijppr.Human, 2025; Vol. 31 (12):363-371.
Conflict of Interest Statement: All authors have nothing else to disclose.